Journal of Cleaner Production 430 (2023) 139441

Contents lists available at ScienceDirect

Journal of Cleaner Production

journal homepage: www.elsevier.com/locate/jclepro

Multi-objective optimization of flexible pavement design from an environmental and economic perspective

Abrohom Demir [a], Joao Santos [b,*], Seirgei Miller [b], Ronald Diele [c], Gijs Naarding [a]

[a] Twentse Weg-en Waterbouw B.V., 7621 BA, Borne, the Netherlands
[b] Civil Engineering and Management Department, Faculty of Engineering Technology, University of Twente, Drienerlolaan 5, 7522 NB, Enschede, the Netherlands
[c] ReintenInfra B.V., 7621 BA, Borne, the Netherlands

ARTICLE INFO

Handling Editor: Zhen Leng

Keywords:
Flexible pavement design
Multi-objective optimization
Genetic algorithm
Environmental impacts
Construction costs
Pavement performance criteria

ABSTRACT

In recent years, construction companies have been pressured by clients to deliver infrastructure that are not only affordable, but also more environmentally friendly. Flexible road pavements are an example. These are multi-layered systems where each layer has its own type of mixture and thickness. The number of asphalt mixtures available to contractors is increasing in size, creating a wide range of flexible pavement design alternatives. These increases make it difficult for the pavement designer to find simultaneously the most affordable and environmentally friendly design, while also ensuring that pavement performance requirements are met. This paper employs a multi-objective optimization (MOO) approach that uses the weighted sum method and genetic algorithm (GA) to find optimal pavement designs by minimizing the Environmental Costs Indicator (ECI) alongside construction costs. The MOO approach was applied to five different pavement design settings, including a real-life case study, to find optimal solutions for each setting. This approach enables the reduction of both ECI and construction costs of pavement designs comparatively with those made by the pavement designer. We recommend that the design responsibility of flexible pavements be handed over from client to contractor to prevent the design of pavement structures that result in unnecessary environmental impacts and costs.

1. Introduction

It is no secret that a well-connected road network plays an important role in improving the economy of a country by enabling the efficient transportation of goods, people and services. Consequently, local, regional and national governmental bodies are willing to invest large sums of financial resources in their road network to ensure that their economies can improve. Since road networks predominantly consist of flexible pavements, these types of asphalt-paved surfaces can be considered as the main culprit impacting road network costs.

In addition to the large cost involved, the construction of flexible pavements is also an environmentally damaging process (Espinoza et al., 2019). As a result, while clients demand that pavement performance requirements are met, they are increasingly pressuring contractors to minimize both costs and environmental impacts during the production, transportation and construction stages of flexible pavements. Bid assessments now deviate from the traditional cost-based approach to one that includes environmental aspects in the bidding criteria (Garbarino et al., 2016).

One promising way to enable affordable and environmentally friendly flexible pavement structures is to optimize the pavement design process. Multi-layered flexible pavement structures can consist of up to seven layers, where the design considers the type of mixtures and thickness assigned to each layer as variables (Abaza, 2021). The number of alternative designs depends on the range of mixtures a contractor has access to. The numbers involved can be large, making it difficult for a human decision-maker (DM) to find the most environmentally friendly and cheapest option that still meets pavement performance requirements.

Usually, pavement performance requirements are determined by the bottom-up fatigue cracking caused by the horizontal tensile strain at the bottom of the asphalt layers and the permanent deformation caused by a vertical compressive strain on top of the subgrade layer (Strickland, 2015). Traditional design methods, as described in The Bitumen Shell Handbook (Huang, 2004; Strickland, 2015; Vasudevan et al., 2015), are commonly used to ensure that critical strain values are not exceeded. These methods are an iterative and trial-and-error way of determining the structure of a flexible pavement that satisfy these performance

* Corresponding author.
E-mail address: j.m.oliveiradossantos@utwente.nl (J. Santos).

https://doi.org/10.1016/j.jclepro.2023.139441
Received 29 January 2023; Received in revised form 25 August 2023; Accepted 20 October 2023
Available online 27 October 2023

requirements. Further, there is not an integrated approach that simultaneously accounts for costs and environmental impacts. As such, a sub-optimal design is frequently selected over a cheaper and more environmentally sound design.

Optimization studies have assessed the effect of layer resilient moduli and thicknesses on pavement performance (Peddinti et al., 2020; Saride et al., 2019). The reliability of the design based on rutting and fatigue failure was optimized for a four-layered flexible pavement system by varying layer moduli and thicknesses. An analysis was made on which layer properties were deemed to influence pavement performance reliability significantly. Sahis and Biswas (2021) considered a three-layered flexible pavement system and attempted to optimize the thickness of both the bituminous and unbound sub-base layer in order to improve pavement performance. This was done using Boussinesq's theory and Odemark's method (Odemark, 1949) to determine the critical strains and transform the three-layered system into a homogenous system, respectively.

In addition to the exclusive consideration of pavement performance in optimization approaches, the scientific community has steadily adopted a more integrated approach using cost models as the objective function to be minimized (Abaza and Abu-Eisheh, 2003; Mamlouk et al., 2000). Rajbongshi and Das (2008) adopted such an approach to minimize costs, while also meeting pavement performance reliability requirements. The development of cost-effective design charts depicting optimal layer thicknesses proved to be an improved methodology when compared to traditional flexible pavement design methods. Gaurav et al. (2011) integrated a costs-based model with pavement performance constraints based on the Mechanistic-Empirical Pavement Design Guide (MEPDG). This led to optimized layer thicknesses. Similarly, Ghanizadeh (2016) optimized the flexible pavement layer configuration and thicknesses for costs minimization, while also adhering to Iranian design code. Other optimization studies have been performed to minimize costs and to meet design criteria for rigid (Hadi and Arfiadi, 2001) and flexible pavement design (Pryke et al., 2006). Both these studies showed that construction costs can be reduced, while still meeting pavement performance criteria.

Another literature stream addresses the joint optimization of pavement design and maintenance and rehabilitation (M&R). In this context, McDonald and Madanat (2012) proposed a life-cycle cost optimization model for mechanistic-empirical (M-E) pavement design. Here, the objective is to minimize the sum of the initial construction and future maintenance costs. The maintenance method they assumed was limited only to resurfacings and the optimal pavement design was determined by nonlinear mathematical programming.

Lee and Madanat (2014) also proposed a methodology for the joint optimization of pavement design and M&R strategies. Their objective was to minimize the net present value of discounted life cycle costs over an infinite time horizon. This included initial construction costs, agency investments for maintenance activities and resurfacings, and user cost. Further, no distinction was made between the different pavement layers and mixtures, as the total structural number was the only decision variable related to the pavement structure. Similarly, Bai et al. (2015) developed a pavement design and rehabilitation optimization framework based on the M-E analysis of pavement response and performance prediction. A finite horizon, single pavement design and rehabilitation problem was formulated to address the trade-off between agency and user costs. A dynamic programming approach was used to solve the optimization problem to minimize the net present value of the life cycle cost. This consisted of agency and user costs over the planning horizon.

The consideration of cost models in the objective function of system reliability-based design optimization (SRBDO) of flexible pavements has also been explored by the research community. Sanchez-Silva et al. (2005) presented such a model based on economic and operation considerations. Dilip and Babu (2021) developed this type of approach to determine optimal layer thicknesses that lead to low costs, while maintaining acceptable pavement reliability levels for fatigue and rutting. More recently, Dilip and Babu (2023) developed a SRBDO approach to define the optimum combination of pavement layer thicknesses and moduli that meet the target levels of reliability, given the expected traffic demand and subgrade strength at a pavement site. They relied on surrogate models to speed up the reliability estimation, as well as the global optimization process.

The literature reviewed above makes clear that the current state of the optimization-based flexible pavement design approaches focuses only on costs and pavement performance. These are ill-prepared to accommodate the new and pressing needs of contractors who see in the minimization of the environmental impacts of their flexible pavement construction projects an opportunity to leapfrog directly to address the needs of a greener construction sector. Despite such developments, no optimization study yet has attempted to fill this gap in knowledge. Hence, a constrained multi-objective optimization (CMOO) approach is needed that considers the concomitant minimization of construction costs and environmental impacts, while ensuring that pavement performance requirements are met. This approach would enable the selection of mixtures and thicknesses used in each layer to reach a globally optimal pavement design for any given traffic volume.

Thus, the objectives of the research work presented in this paper are twofold: (1) to develop a CMOO approach for the design of flexible pavement structures that considers costs, environmental impact indicators and pavement performance requirements. This using the Dutch context as an example; and, (2) to propose optimal flexible pavement structures that meet performance requirements at the lowest construction costs and environmental impacts scores for different traffic volumes.

The following outline is used to achieve these objectives. Section 2 presents the model formulation used by the solution method. This describes the mathematical formulations of the objective functions and constraints. Section 3 elaborates on the solution method used to solve the CMOO problem. Section 4 presents the pavement design settings and sensitivity analysis to illustrate and give context to the applicability of the proposed approach. Section 5 details the results of the application of the CMOO approach to the pavement design settings and sensitivity analysis. These are discussed in Section 6. Finally, Section 7 provides concluding remarks on the main advancements presented in this paper.

2. Constrained multi-objective optimization (CMOO) model formulation

The proposed CMOO approach for the flexible pavement design problem described in this paper consists of several models and component to calculate the objective functions values and constraints as illustrated in Fig. 1. Further details on the several models and components are presented in later sub-sections.

2.1. Nomenclature

The abbreviations used for outlining the model formulation and respective definition can be found in Table 1.

2.2. Decision variables

The flexible pavement design can be changed by varying the thickness and mixture of each layer. In the Netherlands, the design of a flexible pavement can consist of up to six asphalt layers. Usually, one subbase layer is added in between the subgrade layer and the asphalt structure (Bouman et al., 2012). The natural subgrade layer is fixed and, therefore, is not considered a decision variable. Since each of the seven layers can have both a thickness and mixture assigned to it, the decision vector $\vec{X}$ consists of 14 decision variables, each being represented by a real number. In mathematical language, $\vec{X} \subset \mathbb{R}^n$ with n being equal to 14.

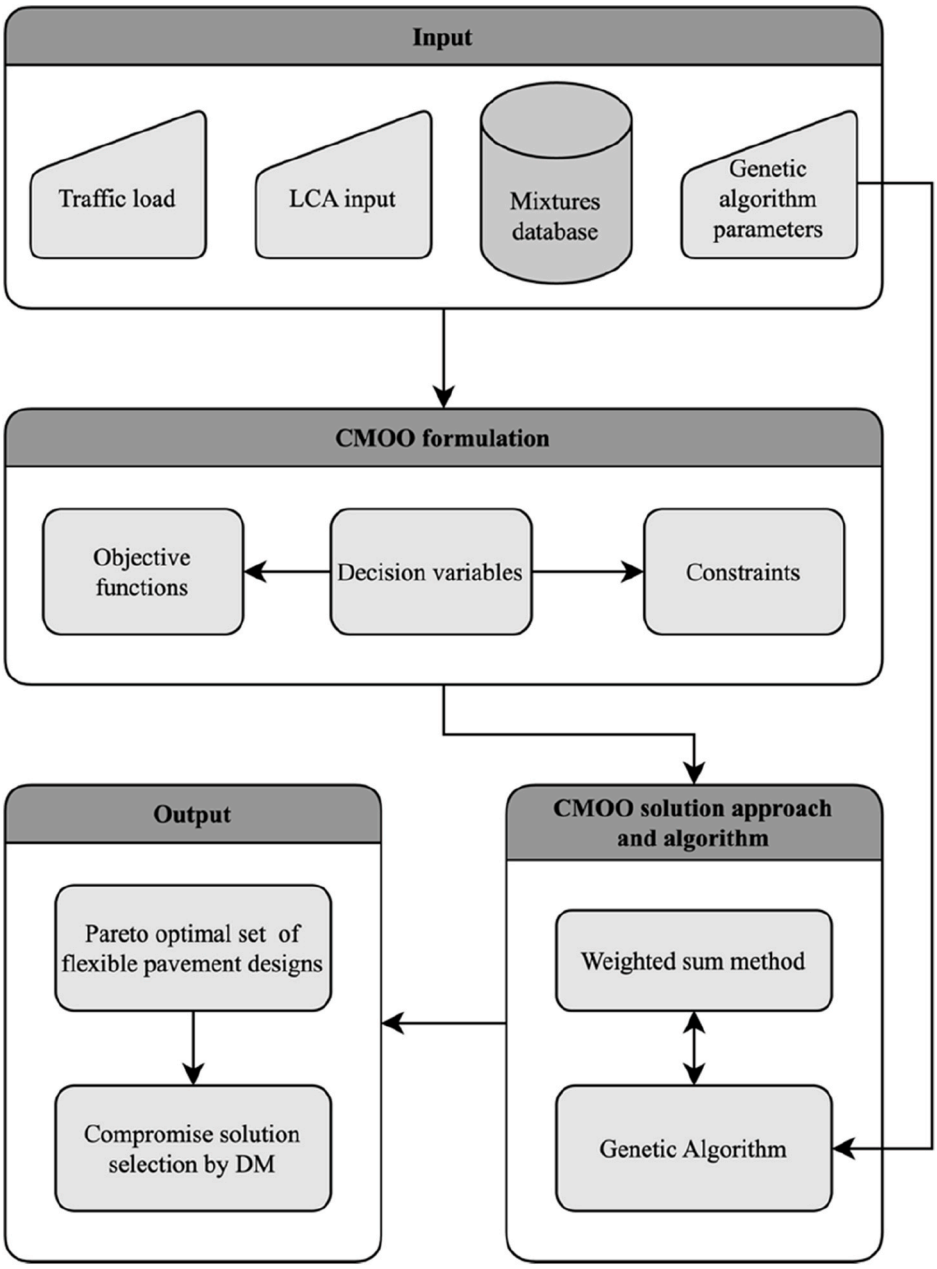

Fig. 1. Architecture of the CMOO approach for the flexible pavement design problem.

2.3. Objective functions

The two objective functions to be minimized in the CMOO approach are the cradle-to-laydown environmental impacts and corresponding costs of the Dutch flexible pavement construction process. The mathematical formulation is elaborated upon in this section.

2.3.1. Minimization of the environmental cost indicator (ECI)

The environmental impact minimization is based on the Environmental Costs Indicator (ECI) methodology described by de Bruyn et al. (2017). The ECI expresses all environmental impacts as one single value in euro per ton. More specifically, it corresponds to the costs of preventive measures for the government to avoid these environmental impacts. Examples of impact categories include: climate change (€/kg CO_2-eq.), ecotoxicity (€/kg 1,4 DB-eq.), acidification of soil and water (€/kg SO_2-eq.), ozone depletion (€/kg CFC-11-eq.), amongst others. The ECI methodology can be seen as a weighting methodology of the impact assessment stage of a typical Life Cycle Assessment (LCA) study. The weighting factors used in the Netherlands are the so-called ECI weights, which are based on the shadow price methodology. Once quantified, the environmental impacts of a product are multiplied by their respective ECI weights and summed. The resulting value is the ECI. The system boundaries of the LCA study underlying to the calculation of the present objective function only comprise the phases A1–A5 (Fig. 2).

The Dutch asphalt sector incorporates the ECI methodology in the Product Category Rules for asphalt mixtures also known as NL-PCR Asfalt 2.0 (Van der Kruk and Overmars, 2022). This report contains the methodology that explains how ECIs are calculated for asphalt mixtures by using Environmental Product Declarations (EPDs) within the Ecochain software (Ecochain Helix, 2022). The ECI related to the production stages (i.e., A1-A3) are retrieved from the Ecochain software. In turn, the ECI related to the transportation and construction stages, (i.e., A4 and A5, respectively) are retrieved from Bak et al. (2022). This shows average ECI values for the different LCA stages per mixture in the

Table 1
Nomenclature adopted in the formulation of the CMOO approach for the flexible pavement design problem.

Abbreviation	Definition (unit)	Abbreviation	Definition (unit)
Objective functions			
ECI	Environmental Costs Indicator of the pavement designs ($euro/m^2$)	C	Construction costs of the pavement designs ($euro/m^2$)
ECI_i^{A1-3}	The *ECI* for LCA stages A1, A2 and A3 for the mixture used in layer i ($euro/ton$)	C_i^{A1-3}	Costs of LCA stages A1, A2 and A3 for the mixture used in layer i ($euro/ton$)
ECI^{A4}	The *ECI* for LCA stage A4 ($euro/tkm$). Linearly deduced from Bak et al. (2022)	C^{A4}	Costs of LCA stage A4 ($euro/tkm$)
ECI_i^{A5}	The *ECI* for LCA stage A5 for the mixture used in layer i according to Bak et al. (2022) ($euro/ton$)	C^{A5}	Costs of LCA stage A5 ($euro/day$)
L	Number of layers in the pavement structure, where the maximum value is equal to 7 (−)	i	Layer number with $i = 1$ being the surface layer and $i = 7$ being the subbase layer (−)
h_i	Thickness of layer i (m)	ρ_i	In-situ density of layer i ($tonnes/m^3$)
D_i	Transportation distance from the plant where the mixture used in layer i is produced to the project location (km)	R_i	Construction rate for the mixture used in layer i according to Bak et al. (2022) ($tonnes/day$)
Constraints			
TI	Truck intensity in one direction ($trucks/day$)	v	Vehicle speed (km/h)
PC_{road}	The performance class of the road based on the TI and v (−)	PC_i	The performance class of the mixture in layer i (−). Values are given in Appendix A (also in case of base, binding, or a binding layer underneath porous asphalt).
$h_i^{(L)}$	Lower boundary thickness value of the mixture in layer i (m)	$h_i^{(U)}$	Upper boundary thickness value of the mixture in layer i (m)
M_f^c	Miner's number for fatigue failure that is calculated (−)	M_r^c	Miner's number for rutting failure that is calculated (−)
M_f^a	Allowable Miner's number for fatigue failure (−)	M_r^a	Allowable Miner's number for rutting failure (−)
n_{lj}^f	Number of design load repetitions for fatigue failure for axle load category l and tire configuration j (−)	n_{lj}^r	Number of design load repetitions for rutting failure for axle load category l and tire configuration j (−)
N_{lj}^f	Allowable number of design load repetitions to prevent fatigue failure for axle load category l and tire configuration j (−)	N_{lj}^r	Allowable number of design load repetitions to prevent rutting failure for axle load category l and tire configuration j (−)
SDB_j^f	Relaxation factor for scattered driving behaviour i.e., not all traffic drives over the same spot, for fatigue failure for tire configuration j (−)	SDB_j^r	Relaxation factor for scattered driving behaviour i.e., not all traffic drives over the same spot, for rutting failure for tire configuration j (−)
ε_{lj}^f	Horizontal tensile strain at the bottom of the asphalt structure for axle load category l and tire configuration j ($\mu m/m$)	ε_{lj}^c	Vertical compressive strain at the top of the subgrade layer for axle load category l and tire configuration j ($\mu m/m$)
D_f	Allowable damage factor given by the client to determine M_f^a (−)	H_f	Healing factor against fatigue failure (−)
E_a	Equivalent stiffness of the entire asphalt structure (MPa). It depends on stiffness parameters of each mixture (see Appendix A)	c_1^E	Stiffness coefficient of which there are four in total (−).
T^E	Temperature at the lab when stiffness of a mixture is tested (°C).	f^E	Loading frequency at the lab when stiffness of a mixture is tested (Hz).
CK^E	Experimentally defined constant used in the lab when stiffness of a mixture is tested (K)	AL	Number of axle load categories, where the maximum value is equal to ten (−)
TC	Number of tire configurations, where the maximum value is equal to four (−)	l	Axle load category (−)
P_l	Contribution of axle load category l to N_d (%)	j	Tire configuration category (−)
N_d	Total number of design load repetitions (−)	P_j	Contribution of tire configuration j to N_d (%)
T	Percentage of trucks in the ADT (%)	ADT	Average daily traffic (veh/day)
W	Number of working days that the road is active ($days$)	a_{axle}	Average number of axles on a single truck (−)
L_f	Lane distribution factor of truck traffic (−)	Dir_f	Directional distribution factor of truck traffic (−)
t	Design life of the flexible pavement design ($years$)	G_f	Growth factor of truck traffic over the entire design life of the road (−)
U	Correction factor for uncertainty in counting data (−)	v_f	Correction factor for traffic speed (−)

Dutch asphalt sector by using a representative asphalt plant and pavement project location. These ECI values are used by default by contractors when specific A4 or A5 ECI values are not available. This is also the case in the CMOO problem described in this paper. The ECI objective function is mathematically expressed in Eq. (1).

$$Minimize\ ECI = \sum_{i=1}^{L} h_i \times \rho_i \left(ECI_i^{A1-3} + ECI^{A4} \times D_i + ECI_i^{A5} \right) \quad (1)$$

2.3.2. Minimization of construction costs

Similarly, the cost minimization of the construction process of flexible pavements is also based on the production, transportation and construction stages, i.e. A1 until A5 (Fig. 2). The construction rate per mixture ($tonnes/day$) for the cost calculation of stage A5 is retrieved from Bak et al. (2022). The cost objective function is mathematically expressed in Eq. (2).

$$Minimize\ C = \sum_{i=1}^{L} h_i \times \rho_i \left(C_i^{A1-3} + C^{A4} \times D_i + \frac{C^{A5}}{R_i} \right) \quad (2)$$

2.4. Constraints

The Dutch context for the design of flexible pavements follows the guidelines proposed by Bouman et al. (2012). They intended to help the pavement designer in designing flexible pavements that cope with common flexible pavement failure mechanisms. These guidelines can be seen as the Dutch equivalent of the AASTHO method (AASTHO, 1993). The optimization constraints in the proposed methodology accord with these guidelines, unless specifically mentioned otherwise. There are three constraints to be discussed in this section: (1) decision variable constraints, (2) the constraint related to bottom-up fatigue cracking, and (3) the constraint related to rutting.

2.4.1. Decision variable constraints

The Dutch asphalt sector considers four standard traffic classes based on the daily truck intensity (TI) and the traffic speed (v) (CROW, 2020). These are presented in Table 2. Each traffic class represents the so-called performance class of the road (PC_{road}) (Eq. (3)). Asphalt mixtures are also assigned performance classes (PC_i) that indicate whether they can be used in a given pavement structure. The complete dataset of all mixtures and their PCs considered in the pavement design settings used

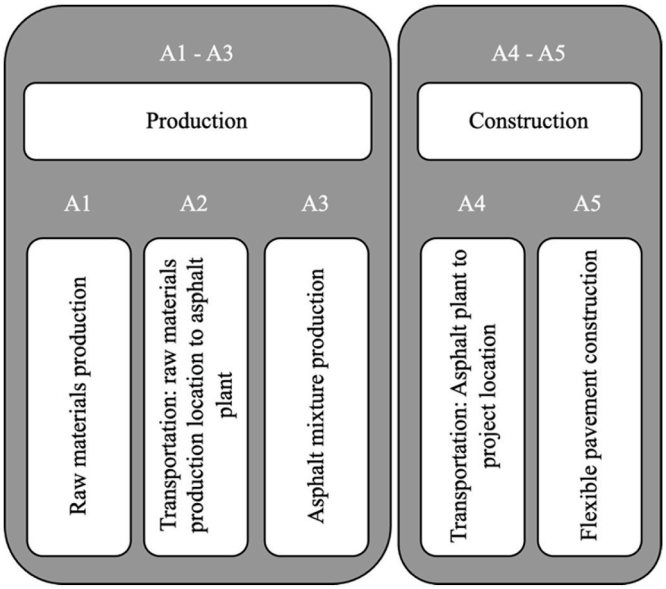

Fig. 2. System boundaries of the LCA considered in the CMOO approach for the flexible pavement design problem.

to illustrate the proposed CMOO approach presented in this paper are shown in Appendix A.

$$PC_{road} \in \{PC_1, \ldots, PC_4\} \tag{3}$$

The order in which layers are presented is important for the validity of the design of flexible pavement structures. Typically, flexible pavement structures consist of at least a surface, base and subbase layer, in that order. The compulsory layers, their order and required data are shown in Table 3.

Finally, each mixture is allowed to have a certain thickness ranging between a lower and upper boundary. This is based on the Dutch asphalt pavements design specifications (Rijkswaterstaat, 2016), henceforth, referred to as SOA. The dataset in Appendix A shows these boundaries, which are mathematically described in Eq. (4).

$$h_i^{(L)} \leq h_i \leq h_i^{(U)}, \forall i \in L \tag{4}$$

2.4.2. The bottom-up fatigue cracking failure constraint

The pavement structure in the optimization approach is subject to a range of different axle loads and tire configurations (ALTC) that amount to 40. The damage contribution of each combination to the pavement performance can be calculated and combined with all the other configurations using Miner's law (Miner, 1945).

For bottom-up fatigue cracking, the horizontal tensile strain at the bottom of the asphalt pavement structure needs to be calculated for every ALTC. For this purpose, the Adaptive Layered Viscoelastic Analysis (ALVA) model is used (Skar and Andersen, 2020). The ALVA model allows the calculation of the pavement response at any given point within the pavement, making it suitable for the optimization of the design of flexible pavement structures.

Miner's law, in the context of bottom-up fatigue cracking failure and how it relates to the tensile strain at the bottom of the asphalt structure, is mathematically expressed in Eqs. (5)–(10). For definitions and units of each parameter, the reader is referred to Section 2.1. In these equations, Eq. (5) ensures that the calculated Miner's number for fatigue failure does not exceed the allowed Miner's number. Eq. (6) defines the allowed Miner's number based on the allowable damage factor defined by the pavement designer. Eq. (7) represents the calculation of the Miner's number for a given pavement structure. Eq. (8) describes the calculation of the number of design load repetitions for fatigue failure. Eq. (9) defines the allowable number of design load repetitions. Finally, Eq. (10) describes the total number of design load repetitions.

$$M_f^c \leq M_f^a \tag{5}$$

$$M_f^a = \frac{1}{0.75 \times 10^{0.38 \times D_f}} \tag{6}$$

$$M_f^c = \sum_{l=1}^{AL} \sum_{j=1}^{TC} \frac{n_{lj}^f}{N_{lj}^f}, \forall l \in AL, \forall j \in TC \tag{7}$$

$$n_{lj}^f = P_l \times P_j \times N_d \times SDB_j^f, \forall l \in AL, \forall j \in TC \tag{8}$$

$$N_{lj}^f = H_f \times \exp\left(c_1^f + c_5^f \times \left\{\ln\left[\varepsilon_{lj}^t\right] + c_2^f \times ln^2[E_a] + c_3^f \times \ln[E_a] + c_4^f\right\}^2\right), \quad \forall l \in AL, \forall j \in TC \tag{9}$$

$$N_d = ADT \times T \times a_{axle} \times W \times Dir_f \times L_f \times G_f \times t \times v_f \times U \tag{10}$$

2.4.3. The rutting failure constraint

Similarly, the rutting constraint is also calculated using Miner's law. Instead of the horizontal tensile strain at the bottom of the asphalt pavement structure, the rutting constraint requires the ALVA model to calculate the vertical compressive strain on top of the subgrade layer. The relation between Miner's law and the vertical compressive strain on top of the subgrade layer is mathematically expressed in Eq. (11)–(15), where Eq. (11)–(14) are the rutting failure counterpart of Eqs. (5)–(8). The allowable number of design load repetitions per ALTC for the rutting constraint is determined following Eq. (15). This is calculated using the vertical compressive strain on top of the subgrade layer.

$$M_r^c \leq M_r^a \tag{11}$$

$$M_r^a = 1 \tag{12}$$

$$M_r^c = \sum_{l=1}^{AL} \sum_{j=1}^{TC} \frac{n_{lj}^r}{N_{lj}^r}, \forall l \in AL, \forall j \in TC \tag{13}$$

$$n_{lj}^r = P_l \times P_j \times N_d \times SDB_j^r, \forall l \in AL, \forall j \in TC \tag{14}$$

$$N_{lj}^r = 10^{\left(17.289 - 4 \log\left(\varepsilon_{lj}^c\right)\right)}, \forall l \in AL, \forall j \in TC \tag{15}$$

Table 2
Dutch traffic classes.

Truck intensity (*TI*) (trucks/day)	Traffic speed (v) (km/h)	PC_{road}
$TI < 50$	$v > 15$	1
$50 \leq TI \leq 2500$	$v > 15$	2
$TI > 2500$	$v > 15$	3
$TI > 250$	$v \leq 15$	4

3. Solution method

3.1. The constrained multi-objective optimization (CMOO) approach

Although the ECI and cost objective functions are expressed in the same unit, the simple addition of objectives to create a single objective optimization (SOO) problem is not correct. The reason being is that both objectives are valued differently i.e., 1 EUR in construction costs is not equal to 1 EUR in ECI, since each client values the ECI differently during the bidding procedure and these values also change over time. Instead, an adequate MOO approach is needed to provide a solution method to evaluate the fitness of potential solutions based on both objectives.

Since the DM will put a certain emphasis on each objective function, preference-based MOO approaches are suitable for the flexible pave-

Table 3
Layer order and required data for constraint violation calculations.

Layer no.	Layer type	Compulsory	Thickness	Stiffness parameters	Fatigue parameters	Poisson's ratio
1	Surface	X	X	X		X
2	Bind		X	X		X
3	Base		X	X		X
4	Base		X	X		X
5	Base		X	X		X
6	Base	X	X	X	X	X
7	Subbase	X	X	X[1]		X
8[2]	Subgrade (sand)	X		X[1]		X

[1] For subbase and subgrade stiffness, a single value is assumed in MPa. No stiffness calculation based on parameters is needed.
[2] Subgrade layer type and thickness are not considered as decision variables, since they are always present and pre-established in practice. Thickness of the subgrade is fixed, as it is always assumed to be infinite.

ment design problem. For this reason, the weighted sum method (WSM) is chosen, as it can account for preference information, both before and after solving the flexible pavement design problem, making it an *a priori,* as well as an *a posteriori,* method (Miettinen, 2008, 2012). The *a priori* version can be used, if the DM is sure about the weights to be assigned to the objective functions, whereas the *a posteriori* version determines, firstly, the Pareto Front (PF), by calculating the objective functions scores over several weighting sets, after which the DM can analyse the trade-offs between objective functions scores by looking at the PF. In a nutshell, the WSM transforms the MOO problem into a SOO problem. The SOO translation by using the WSM is mathematically expressed in Eq. (16). Here, K is the total number of objective functions, k is objective function in question, w_k is the weight applied to objective function k, $f_k^{'}$ is the normalized score of objective function k, $\vec{X}$ is the decision variable vector and S is the feasible solution search space. This equation aims to find a feasible solution, such that the weighted sum of the objectives is minimized for a given weighting set.

$$\begin{aligned} &Minimize: \sum_{k=1}^{K} w_k \times f_k^{'}\left(\vec{X}\right) \\ &subject\ to: \vec{X} \in S \\ &w_k \geq 0, k = 1, \ldots, K, \sum_{k=1}^{K} w_k = 1 \end{aligned} \tag{16}$$

The model formulation is computationally expensive, in particular, the calculation of the critical strain values through the ALVA model. The computational load can be reduced by increasing the step size between the different weight sets. Therefore, the step size of 0.1 was chosen.

Since the different objective functions might be of different orders of magnitude, it was necessary to normalize their scores (Deb, 2001). By minimizing and maximizing each objective separately i.e., with an extreme weight set, the normalization boundaries (i.e., 0–1) can be obtained. The normalized score for each objective function were obtained using Eq. (17). Here, f_k is the score of objective function k and, f_k^{min} and f_k^{max} are the absolute objective scores when minimizing and maximizing objective function k, respectively. The normalized objective score was calculated by dividing the difference between the objective score and the minimum objective score over the difference between the maximum and minimum objective score.

Finally, the formulation of the CMOO model was written in MATLAB® programming software (Matlab R2021b, 2021).

$$f_k^{'}\left(\vec{X}\right) = \frac{f_k\left(\vec{X}\right) - f_k^{min}}{f_k^{max} - f_k^{min}} \tag{17}$$

3.2. Solution algorithm

Many real-life MOO problems consist of non-differentiable or discontinuous functions, making it very difficult for exact algorithms not to fall in local optima (Deb, 2001; Sivanandam and Deepa, 2008). Additionally, other studies have argued that these real-life problems are highly complex and difficult for exact algorithms to solve (Talbi, 2009; Yu and Gen, 2010). Consequently, the use of metaheuristic algorithms in such cases is favoured. Hence, for the CMOO flexible pavement design problem described in this paper, metaheuristics will be applied.

Within the category of metaheuristics, a wide variety of optimization algorithms exist, e.g., Genetic Algorithm (GA), Particle Swarm Optimization (PSO), Simulated Annealing (SA), to name a few. These are also called evolutionary algorithms (EA). The comparison between EA and their variants has proven to be difficult and a choice for one specific EA variant can never be fully justified (LaTorre et al., 2020). Since GA is particularly easy to use and has broad applicability (Deb, 2001), including in the pavement sector (Ferreira and Santos, 2012; Santos et al., 2016, 2017a, 2017b, 2018), the approach proposed in this paper, GA, will also be applied to solve the CMOO flexible pavement design problem. Its working mechanism is illustrated in Fig. 3 and described in the upcoming sub-sections, whereas the adopted parameters are summarized in Table 4.

3.2.1. Population initialization

GA implements a stochastic search procedure to find the global optimal solution. The first step is to initialize the population randomly based on the decision variable constraints. In doing so, a population with N solution individuals is created.

3.2.2. Selection method

The second step consists of selecting the parents to go through the recombination stage. The idea behind the selection step is to stimulate the reproduction of fit parents with the objective of producing even fitter offspring. Tournament selection was chosen as the selection method because it is used in NSGA-II (Deb et al., 2002). This is a widely used GA variant. The steps of tournament selection are described below:

1. Calculate the weighted sum objective function value of each parent.
2. Calculate the constraint violation (CV) using Eqs. (18) and (19).

$$CV\left(\vec{X}\right) = \sum_{z=1}^{Z} \overline{g}_z\left(\vec{X}\right) \tag{18}$$

$$\overline{g}_z\left(\vec{X}\right) = \frac{g_z\left(\vec{X}\right) - g_z^{min}}{g_z^{max} - g_z^{min}} \tag{19}$$

where $\vec{X}$ is the solution individual, $\overline{g}_z$ is the z^{th} normalized CV. The normalized CV is calculated using a similar approach as described in Eq. (17), but here the normalization boundaries are considered to be those of the population (Deb, 2011).

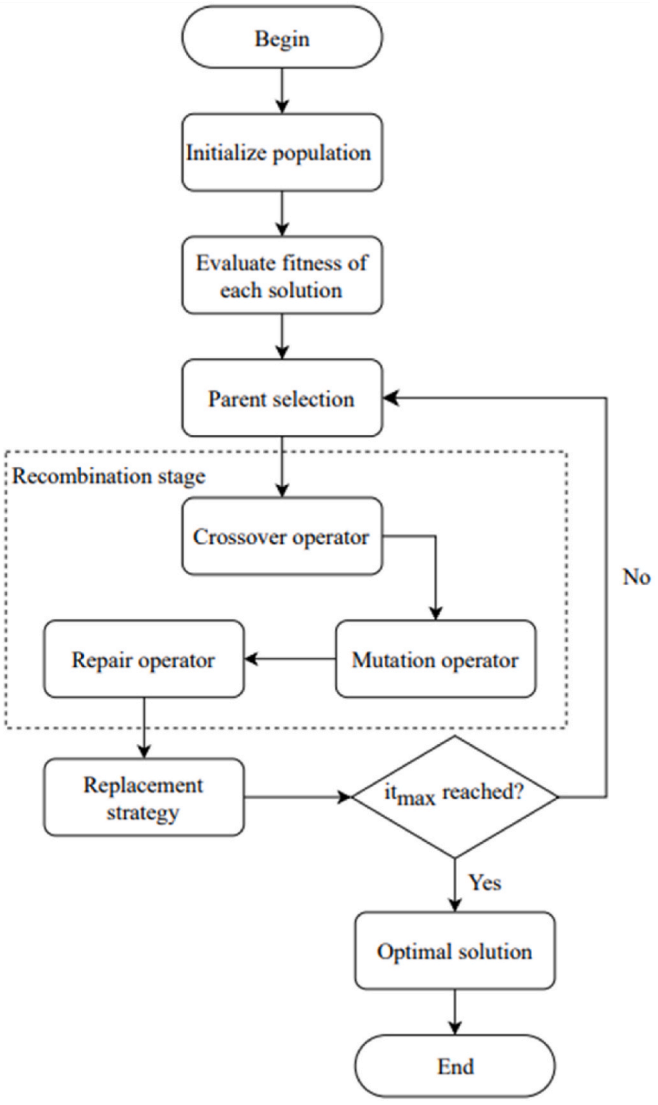

Fig. 3. Working mechanism of GA.

Table 4
Nomenclature adopted for GA parameters of the CMOO flexible pavement design problem.

Abbreviation	Definition
N	Population size
CV	Constraint violation
$\vec{X}$	Decision variable vector, also known as the solution
z	Constraint number
Z	Total number of constraints
$\bar{g}_z$	The z^{th} normalized constraint violation
g_z	The z^{th} absolute constraint violation
g_z^{min}	Lowest z^{th} absolute constraint violation within the population
g_z^{max}	Highest z^{th} absolute constraint violation within the population
T_S	Tournament size for parent selection
P_c	Crossover probability
P_m	Mutation probability
T_R	Tournament size for the replacement strategy
p_e	Elitism preservation operator
it_{max}	Maximum number of iterations

3. Create N tournaments with each tournament having size T_S for parent selection. An increase in T_S, results in higher selection pressure. Additionally, each tournament pool is randomly filled with T_S parents.
4. Determine the winners based on the same approach as proposed in NSGA-II. This includes defining three possible scenarios.
   a. All tournament solutions are feasible solutions, and the winner is selected based on the lowest weighted sum value.
   b. All tournament solutions are infeasible solutions and the solution with the lowest CV is the winner.
   c. Tournament solutions include both feasible and infeasible solutions. Only the feasible solutions can win and among them the solution with the lowest weighted sum value is the winner.
5. Produce parent sets of size two based on tournament winners to go through the recombination stage.

3.2.3. Offspring generation

During the recombination phase, the two parents in each parent set will mate and produce offspring through crossover. Furthermore, the genes of offspring will be changed randomly through the mutation operator. Finally, a repair operator is applied to fix solutions that violate the decision variable constraints, after the crossover and mutation operators have been applied. There are two parameters that influence optimization quality. These are the crossover probability (P_c) and mutation probability (P_m). Offspring generation will occur using the following procedure:

1. The two parents within a parent set will exchange genetic material using single point crossover (SPC). Whether or not crossover will take place between the two parents is based on the P_c. Either way, two offspring individuals are created. As a result, an offspring population of size N is created.
2. The created offspring solutions in step 1 will also be mutated, based on the P_m. Because the decision vector consists only of real numbers and is non-binary, the mutated gene in question will be assigned a random value that meets the decision variable constraints.
3. The crossover and mutation operator can cause invalid solutions to occur (Talbi, 2009). Consequently, a repair operator is used to check for invalid solutions and repairs them afterwards.

For the crossover operator, two-point crossover (TPC) and uniform crossover (UC) were also tested, but resulted in worse optimization quality than SPC. When the order matters in the decision variable vectors, these last two crossover operators are more likely to disrupt fitter chromosomes than to improve their fitness (Reeves, 2010; Sivanandam and Deepa, 2008). Two SPC operators are applied simultaneously and independently on both the mixture type and thickness decision vectors. This way, mixture type and thickness variables for a particular layer are not interlocked. This allows for more breathing room with the intention of finding a more diverse offspring population.

3.2.4. Replacement strategy

At this point, there are two populations i.e., the parent and offspring populations, both of size N. Combining these two populations into one creates a population size of $2N$. Traditional GA maintain a fixed population size, meaning that not all parents and offspring can go to the next generation. For this purpose, a replacement strategy is needed that allows for fitter offspring solutions to replace worse parent solutions. The GA in the proposed approach incorporates a replacement strategy that includes a tournament for each spot in the next generation with tournament size T_R. Additionally, an elitism preserving operator (p_e) is included similarly to the NSGA-II approach. The idea is that during the

replacement process p_eN spots (rounded up) are reserved for the best solutions within that iteration. This way the best solution(s) across all iterations will never get lost. The remaining $N - p_eN$ spots will be filled using the tournament method discussed earlier. All the steps from Section 3.2.2. until 3.2.4 will be repeated for it_{max} iterations.

3.2.5. GA parameters calibration

Traditionally, GAs are computational expensive search algorithms whose quality of the "optimal" solutions depends on the parameter's values adopted. By calibrating the GA parameters, a balance between computational time and optimization quality can be found. The best-found GA configuration for the CMOO flexible pavement design problem discussed in this paper is summarized in Table 5 and was obtained through a combinatorial trial-and-error approach.

4. Illustration of the applicability of the developed CMOO approach

The developed CMOO approach was applied to a total of five pavement designs. Four designs were dedicated to the PCs shown in Table 2, whereas the fifth is a real-life case study for a municipal road in the city of Enschede, The Netherlands.

All pavement designs used the same input parameters as shown in Table 6. The values of the OIA parameters are based on SOA that specifies the values to use if the client's quantification is not provided. The pavement designs are different from each other in terms of, either the *TI*, *v*, plant-project distances, or a combination of those. An overview of the differences between the characteristics of the pavement designs is given in Table 7. The dataset can be found in Appendix A. Due to confidentiality reasons, only the rankings of material properties can be disclosed. Finally, each asphalt mixture can be produced with two types of fuel: natural gas (mixtures 12–22) or green gas (mixtures 1–11). Subbase mixtures (mixtures 23 and 24) are produced using an electricity-based crushing installation. An overview of all the fuel types and respective dataset used for mixture production is given in Table 8.

Furthermore, a sensitivity analysis involving three input parameters is performed for the PC pavement designs. These are the mixture cost (C_i^{A1-3}), transportation distances from asphalt plants (plants 1 and 2), and transportation distances from subbase mixture plants (plant 3). These input parameters are chosen for the sensitivity analysis because they are likely to change in practice. An overview of the sensitivity analysis is given in Table 9.

5. Results

This section presents the results of the application of the CMOO approach to the five pavement designs. They were obtained after running the optimization algorithm on a computational device featuring an Intel® Core™ i7-7700HQ CPU @2.80 GHz, 2808 MHz, 4 Core(s), 8 Logical Processor(s), a NVIDIA® Quadro® M1200, 4 GB VRAM and 16 GB of RAM.

Fig. 4 depicts the thickness of the optimal solutions. Figs. 5–8 show the objective function values in the objective search space. The corresponding objective function and constraint values for each weighting set for pavement designs 1–4 (baseline scenarios) are presented in Table 10. Additionally, these figures depict the SA results of the changed input parameters as described in Table 9. The objective function values related to the SA are presented in Tables 11 and 12 in absolute and relative values, respectively. The optimal solutions in Table 10 are determined

Table 5
Algorithm parameters after calibration.

N	T_S	P_c	P_m	T_R	p_e	it_{max}
100	2	0.95	1/14	16	0.01	35

Table 6
Value of the input parameters for all pavement designs.

OIA input parameters	
Name	Value
Design period	20 years
Active days of road per year	270 days
Average axles per truck	3.5
Correction factor for directional distribution	1
Correction factor for lane distribution	1
Correction factor for uncertainty in counting data	1.75
Annual growth of traffic percentage	3.5 %
Lane width	3 m
Distance from tire to edge of road	0.25 m
Axle load range and distribution	Normal municipal road
Tire configuration distribution	Standard
Allowed damage percentage based on Miner's law	15 %
Confidence level	85 %
Other input parameter	
Transportation ECI from plant to project (ECI^{A4})	8.29×10^{-3} euro/tkm
Transportation cost from plant to project (C^{A4})	0.26 euro/tkm
Construction cost (C^{A5})	6546 euro/day

Table 7
Pavement designs characteristics and baseline scenarios for the sensitivity analysis.

Item name	Pavement design ID				
	1	2	3	4	5
Pavement design type	PC 1	PC 2	PC 3	PC 4	Real-life case study
TI (*trucks*/*day*)	40	1225	3000	500	364
v (*km*/*h*)	50	50	50	10	50
Distance from plant 1 to project (*km*)	50	50	50	50	13.5
Distance from plant 2 to project (*km*)	50	50	50	50	94.9
Distance from plant 3 to project (for subbase mixtures) (*km*)	20	20	20	20	17.7

Table 8
Fuel types and specifications used for mixture production based on the Ecoinvent (2020).

Fuel type	Dataset
Natural gas	XXXX-pro&Aardgas, industrieel gebruik, per m3 (o.b.v. 31,7 MJ Heat, district or industrial, natural gas {Europe, without Switzerland}| heat production, natural gas, at industrial furnace >100 kW | Cut-off, U)
Green gas	Green gas, Ecoinvent v 3.2 cut-off, Natural gas, burned in industrial furnace low-NOx >100kW/RER U replaced with Methane, 96 vol-%, from biogas, high pressure, at consumer/CH U and Biogenic Carbon Dioxide
Electricity	0124-pro&1 kWh, uit stopcontact (o.b.v. Electricity, low voltage {NL}| market for | Cut-off, U)

Table 9
Sensitivity analysis characteristics.

Input parameter	Values tested	Sensitivity analysis (SA) ID
Mixture cost (C_i^{A1-3})	+10%, +20%	1, 2
Transportation distances from plant 1 and 2 to the project site	25 and 75 km	3, 4
Transportation distance from plant 3 to the project site	40 and 60 km	5, 6

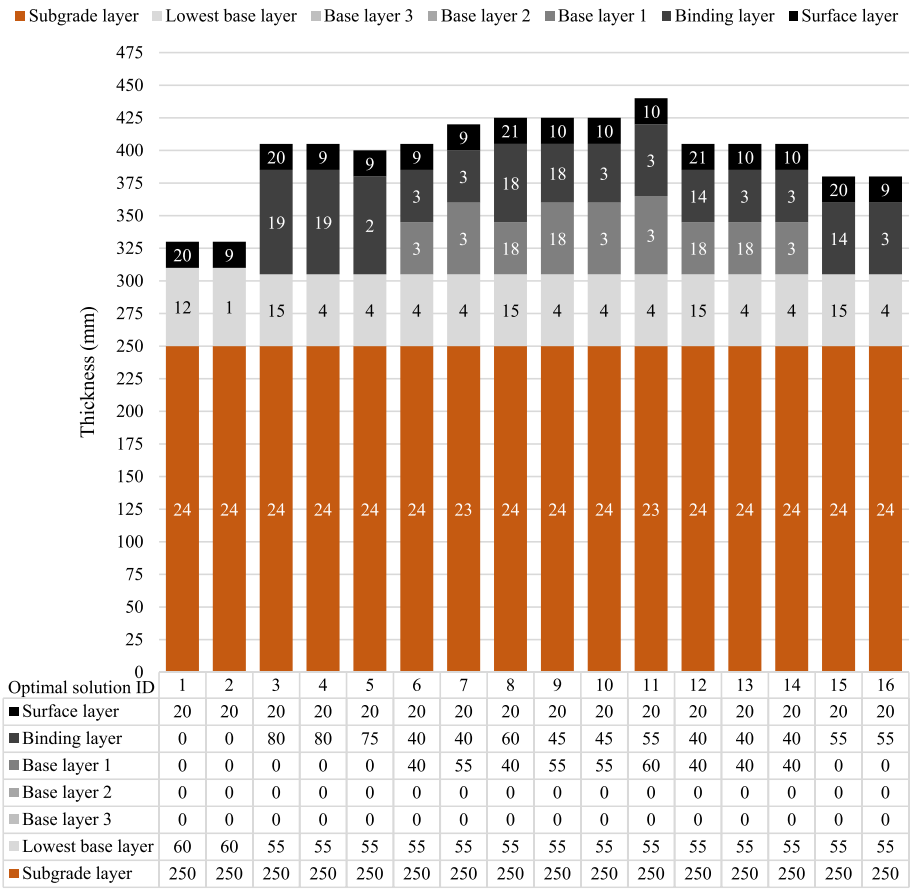

Optimal solution ID	1	2	3	4	5	6	7	8	9	10	11	12	13	14	15	16
Surface layer	20	20	20	20	20	20	20	20	20	20	20	20	20	20	20	20
Binding layer	0	0	80	80	75	40	40	60	45	45	55	40	40	40	55	55
Base layer 1	0	0	0	0	0	40	55	40	55	55	60	40	40	40	0	0
Base layer 2	0	0	0	0	0	0	0	0	0	0	0	0	0	0	0	0
Base layer 3	0	0	0	0	0	0	0	0	0	0	0	0	0	0	0	0
Lowest base layer	60	60	55	55	55	55	55	55	55	55	55	55	55	55	55	55
Subgrade layer	250	250	250	250	250	250	250	250	250	250	250	250	250	250	250	250

Fig. 4. Graphical representation of the optimal solutions. The thickness is shown in y-axis and the mixtures ID at the bottom of the bars.

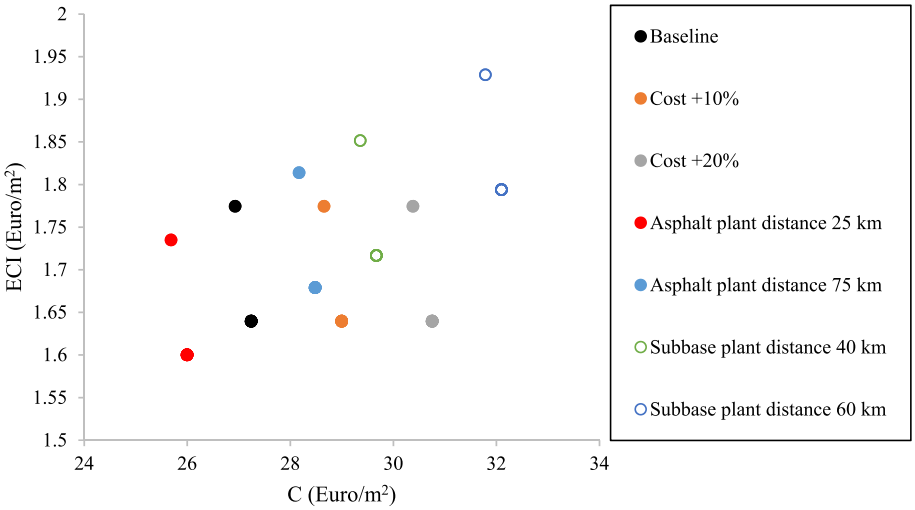

Fig. 5. Optimal solution set of pavement design 1 for baseline and SA of mixture costs, asphalt plant distances and subbase plant distances.

using the GA configuration discussed in Section 3.2.5. The iteration-wise improvement effect of the CMOO approach is depicted in Fig. 10. This considers as an example the generational improvement for ECI weight 0.5 of pavement design 2 (baseline scenario).

From the calculated Miner's numbers for both fatigue and rutting failure, fatigue failure is noted as the most enforcing constraint, since the allowed Miner's numbers (M_f^a and M_r^a) according to Eqs. (6) and (12) are equal to 0.54 and 1, respectively.

The results of the application of the CMOO approach to the real-life case study (pavement design ID number 5) are presented in Fig. 9. This figure also includes the flexible pavement design defined by the pavement designer. Reductions in both objective function values were observed when applying the CMOO approach. These reductions are calculated in relation to the pavement design solution defined by the pavement designer and implemented in the project. The ECI objective function was reduced from 3.34 to 2.35 $euro/m^2$, which corresponds to a reduction of 30%. The C objective function was reduced from 47.33 to 32.83 $euro/m^2$, which corresponds to a reduction of 31%.

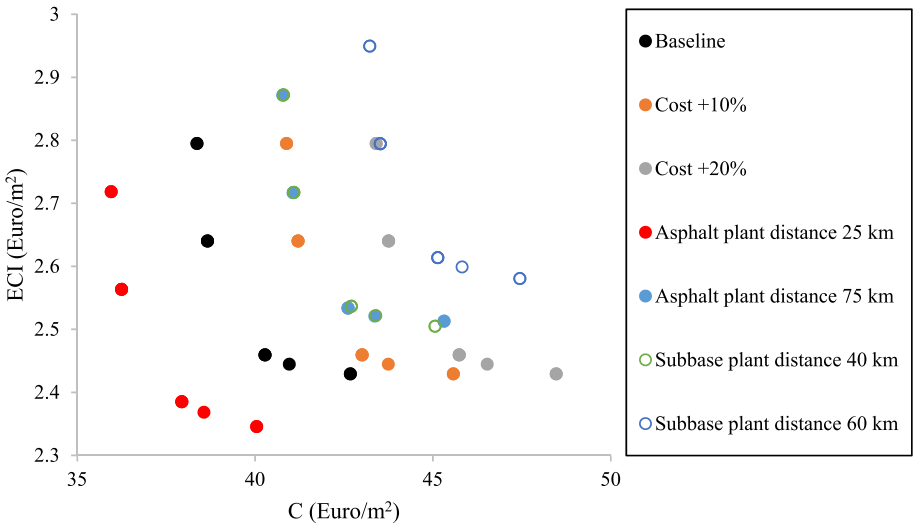

Fig. 6. Optimal solution set of pavement design 2 for baseline and SA of mixture costs, asphalt plant distances and subbase plant distances.

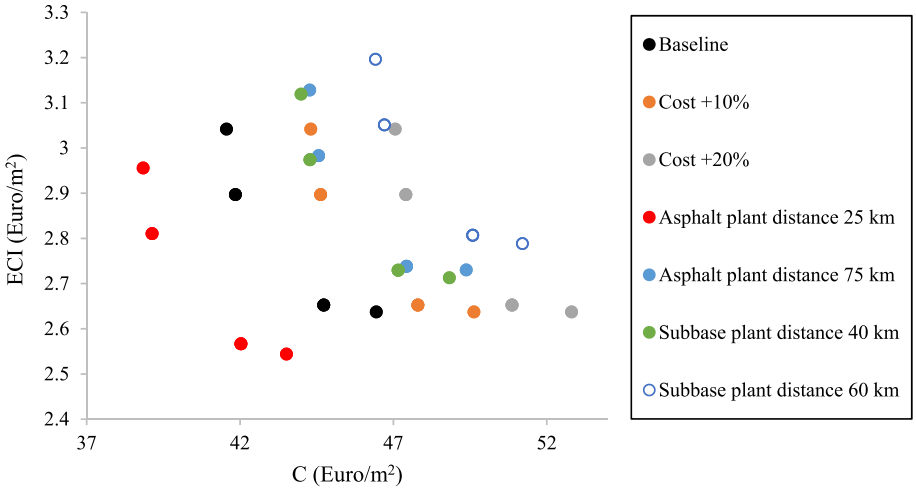

Fig. 7. Optimal solution set of pavement design 3 for baseline and SA of mixture costs, asphalt plant distances and subbase plant distances.

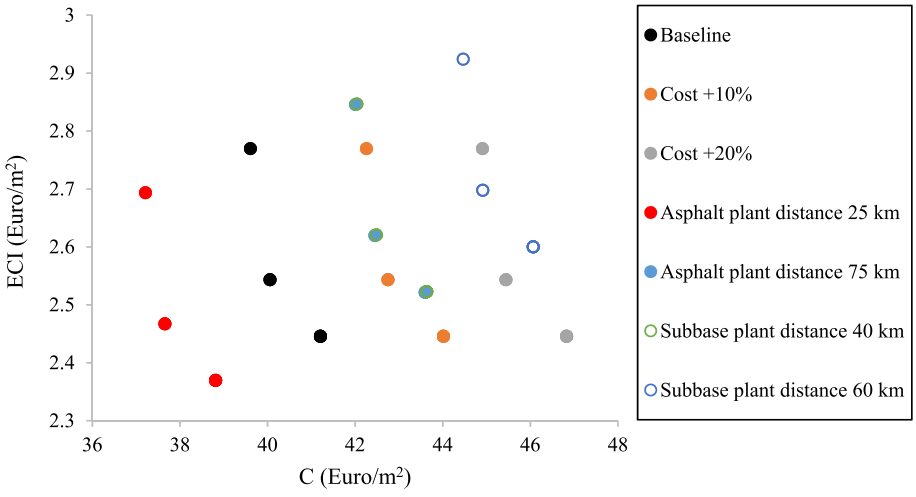

Fig. 8. Optimal solution set of pavement design 4 for baseline and SA of mixture costs, asphalt plant distances and subbase plant distances.

Table 10
Pavement design results showing the sets of optimal solutions.

ECI weights[1]	Pavement design ID	Optimal solution ID[2]	*ECI* (*euro*/*m*²)	*C* (*euro*/*m*²)	*CV*	M_f^c	M_r^c
0–0.1	1	1	1.77	26.93	0	0.5002	0.1272
0.2–1	1	2	1.64	27.24	0	0.5002	0.1272
0–0.1	2	3	2.79	38.37	0	0.4869	0.3219
0.2	2	4	2.64	38.66	0	0.4869	0.3219
0.3–0.5	2	5	2.46	40.28	0	0.5367	0.3420
0.6–0.8	2	6	2.44	40.97	0	0.4470	0.3052
0.9–1	2	7	2.43	42.68	0	0.5279	0.2500
0–0.1	3	8	3.04	41.56	0	0.5164	0.4714
0.2–0.4	3	9	2.90	41.85	0	0.5164	0.4714
0.5–0.8	3	10	2.65	44.73	0	0.4674	0.4419
0.9–1	3	11	2.64	46.45	0	0.5300	0.3595
0–0.1	4	12	2.77	39.61	0	0.5335	0.3036
0.2–0.4	4	13	2.54	40.06	0	0.5335	0.3036
0.5–1	4	14	2.45	41.21	0	0.5314	0.3027
0–0.1	5	15	2.35	32.83	0	0.4499	0.1936
0.2–1	5	16	2.08	33.33	0	0.4499	0.1936

[1] C weights can be obtained by subtracting the ECI weights from 1 as represented by Eq. (16).
[2] The optimal solutions are depicted in Fig. 5 using this ID on the x-axis.

Table 11
Sensitivity analysis objective function values in euro/m^2.

ECI weights	Pavement design ID	SA ID											
		1		2		3		4		5		6	
		ECI	*C*	*ECI*	*C*	*ECI*	*C*	*ECI*	*C*	*ECI*	*C*	*ECI*	*C*
0–0.1	1	1.77	28.66	1.77	30.38	1.73	25.69	1.81	28.17	1.85	29.36	1.93	31.79
0.2–1	1	1.64	29.00	1.64	30.75	1.60	26.00	1.68	28.48	1.72	29.67	1.79	32.10
0–0.1	2	2.79	40.89	2.79	43.40	2.72	35.95	2.87	40.78	2.87	40.80	2.95	43.23
0.2	2	2.64	41.21	2.64	43.76	2.56	36.25	2.72	41.08	2.72	41.09	2.79	43.52
0.3–0.5	2	2.46	43.01	2.46	45.74	2.38	37.94	2.53	42.62	2.54	42.71	2.61	45.14
0.6–0.8	2	2.44	43.75	2.44	46.53	2.36	38.56	2.52	43.37	2.52	43.39	2.60	45.82
0.9–1	2	2.43	45.57	2.43	48.47	2.35	40.05	2.51	45.31	2.50	45.06	2.58	47.44
0–0.1	3	3.04	44.31	3.04	47.06	2.96	38.85	3.13	44.28	3.12	43.99	3.20	46.42
0.2–0.4	3	2.90	44.63	2.90	47.41	2.81	39.14	2.98	44.57	2.97	44.28	3.05	46.71
0.5–0.8	3	2.65	47.80	2.65	50.87	2.57	42.03	2.74	47.43	2.73	47.16	2.81	49.59
0.9–1	3	2.64	49.63	2.64	52.81	2.54	43.52	2.73	49.38	2.71	48.83	2.79	51.21
0–0.1	4	2.77	42.26	2.77	44.91	2.69	37.21	2.85	42.01	2.85	42.04	2.92	44.47
0.2–0.4	4	2.54	42.75	2.54	45.44	2.47	37.66	2.62	42.45	2.62	42.49	2.70	44.91
0.5–1	4	2.45	44.02	2.45	46.83	2.37	38.82	2.52	43.60	2.52	43.64	2.60	46.07

Table 12
Percental change in objective function values relative to the baseline scenarios for the sensitivity analysis.

ECI weights	Pavement design ID	SA ID											
		1		2		3		4		5		6	
		ECI	*C*	*ECI*	*C*	*ECI*	*C*	*ECI*	*C*	*ECI*	*C*	*ECI*	*C*
0–0.1	1	0.00	6.42	0.00	12.81	−2.26	−4.60	2.26	4.60	4.52	9.02	9.04	18.05
0.2–1	1	0.00	6.46	0.00	12.89	−2.44	−4.55	2.44	4.55	4.88	8.92	9.15	17.84
0–0.1	2	0.00	6.57	0.00	13.11	−2.51	−6.31	2.87	6.28	2.87	6.33	5.73	12.67
0.2	2	0.00	6.60	0.00	13.19	−3.03	−6.23	3.03	6.26	3.03	6.29	5.68	12.57
0.3–0.5	2	0.00	6.78	0.00	13.56	−3.25	−5.81	2.85	5.81	3.25	6.03	6.10	12.07
0.6–0.8	2	0.00	6.79	0.00	13.57	−3.28	−5.88	3.28	5.86	3.28	5.91	6.56	11.84
0.9–1	2	0.00	6.77	0.00	13.57	−3.29	−6.16	3.29	6.16	2.88	5.58	6.17	11.15
0–0.1	3	0.00	6.62	0.00	13.23	−2.63	−6.52	2.96	6.54	2.63	5.85	5.26	11.69
0.2–0.4	3	0.00	6.64	0.00	13.29	−3.10	−6.48	2.76	6.50	2.41	5.81	5.17	11.61
0.5–0.8	3	0.00	6.86	0.00	13.73	−3.02	−6.04	3.40	6.04	3.02	5.43	6.04	10.87
0.9–1	3	0.00	6.85	0.00	13.69	−3.79	−6.31	3.41	6.31	2.65	5.12	5.68	10.25
0–0.1	4	0.00	6.69	0.00	13.38	−2.89	−6.06	2.89	6.06	2.89	6.13	5.42	12.27
0.2–0.4	4	0.00	6.71	0.00	13.43	−2.76	−5.99	3.15	5.97	3.15	6.07	6.30	12.11
0.5–1	4	0.00	6.82	0.00	13.64	−3.27	−5.80	2.86	5.80	2.86	5.90	6.12	11.79

6. Discussions

6.1. Optimal solutions

As can be seen in Figs. 5–9, all pavement designs show trade-offs between environmental impacts and construction costs, although to a different extent. The number of optimal solutions per design ranged between two (pavement designs 1 and 5) and five (pavement design 2). Pavement designs 3 and 4 resulted in four and three optimal solutions in the solution set, respectively. Thus, it is up to the decision maker to choose one of the proposed solutions based on his/her preference.

Changing input parameters in the sensitivity analysis has not shown

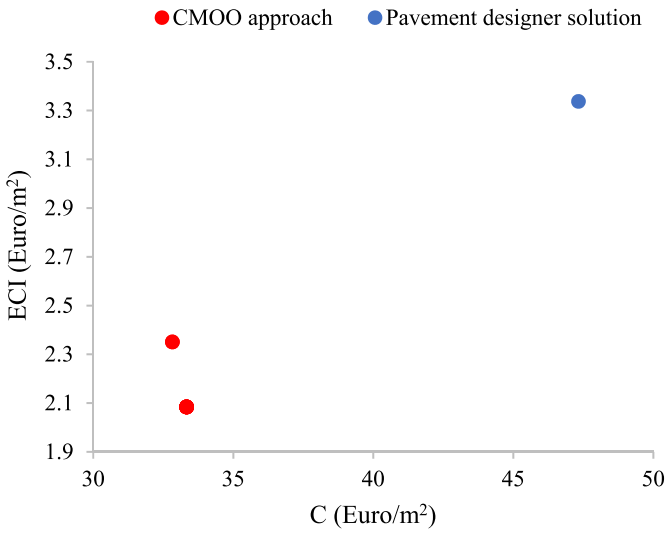

Fig. 9. Optimal solution set of pavement design 5 compared to the pavement designer solution.

they affect the number of optimal solutions, nor did they have any influence on the pavement design. The only change that can be observed are the objective function values. When varying transportation distances for both asphalt and subbase mixtures, construction costs are more affected than environmental impacts. Further, construction costs and environmental impacts associated with thinner asphalt pavement structures, e.g. pavement design 1, are less affected by changes in asphalt plant distances than those of thicker asphalt pavement structures. On the other hand, changes in subbase plant distances affect construction costs and environmental impacts of thinner asphalt pavement structures in a more pronounced way. The reason being that, in the case of thin asphalt pavement structures, subbase layers are responsible for the majority of the quantity of materials to be transported.

Pavement designs 1, 2, 3 and 5 have an increasing traffic volume. This leads to the increase of the thickness of the optimal pavement structures. Note that pavement design 4 also differs in traffic speed and, therefore, cannot be used to determine the relation between traffic volume and optimal pavement structure thickness. However, when comparing pavement designs 4 and 5, it becomes clear that a lower traffic speed with a similar traffic volume requires a thicker pavement structure.

Optimal solutions tend to be characterized by a dominant set of mixtures. Surface mixtures 9, 10, 20 and 21 are alternatively used in all optimal solutions. This can be explained by the fact that surface mixtures have higher costs and ECI values when compared to base/bind mixtures. As such, the algorithm will favour designs with the thinnest surface layers. Within the current dataset the thinnest possible mixtures (20 mm) are the above-mentioned mixtures. Mixtures 11 and 22 can only be 50-mm thick, at the minimum, and are not favoured by the algorithm. Mixtures 9 and 20 are the cheapest and the least environmentally burdensome for PC1 and PC2, whereas for PC3 and PC4 these are mixtures 10 and 21.

Additionally, the lowest-positioned base layer has the highest influence on total pavement thickness, since bottom-up fatigue cracking is initiated in this layer and propagates upwards. The mixture with the best fatigue parameters is predominantly chosen for this layer i.e., mixtures 4 and 15, with the minimum allowed thickness value (55 mm). Similarly, for the surface layer, mixtures 4 and 15 have considerably higher ECI and cost values than the mixtures chosen in other base/bind layers. Therefore, the algorithm favours the lowest-positioned base layer to have the lowest possible thickness. Through selecting mixtures with better fatigue properties for this layer, fatigue cracking criteria can still be met when applying a thinner pavement thickness. This reduces the total pavement thickness. Further, it affects considerably the constructions costs and environmental impacts, and explains why one of the mixtures with the best fatigue characteristics is often chosen, despite it being one of the most expensive base mixtures in the dataset. An exception to this pattern is the pavement design 1. Here mixture 1 or 12 (depending on the weighting set) are selected instead of mixtures 4 or 15. In these cases, the 5 mm that could be reduced from the total pavement thickness is not worth the additional costs and ECI of mixtures 4 or 15 when comparing it to mixtures 1 or 12.

The thickness of subbase mixture of optimal pavement structures is also always set to the lowest possible value, but due to a different reason. ECI and cost values related to the production of subbase mixtures are the lowest, but they contribute the most to the total mass of the pavement structure. Therefore, they have higher transportation and construction ECI and, more importantly, costs. For this reason, the algorithm favours designs with the thinnest possible subbase mixtures. When the weighting set favours ECI, instead of construction costs, subbase mixture 23 is sometimes chosen. When the preferred weighting set favours construction costs instead of ECI, subbase mixture 24 is always chosen.

Mixtures in layers in between the most bottom base and surface layer

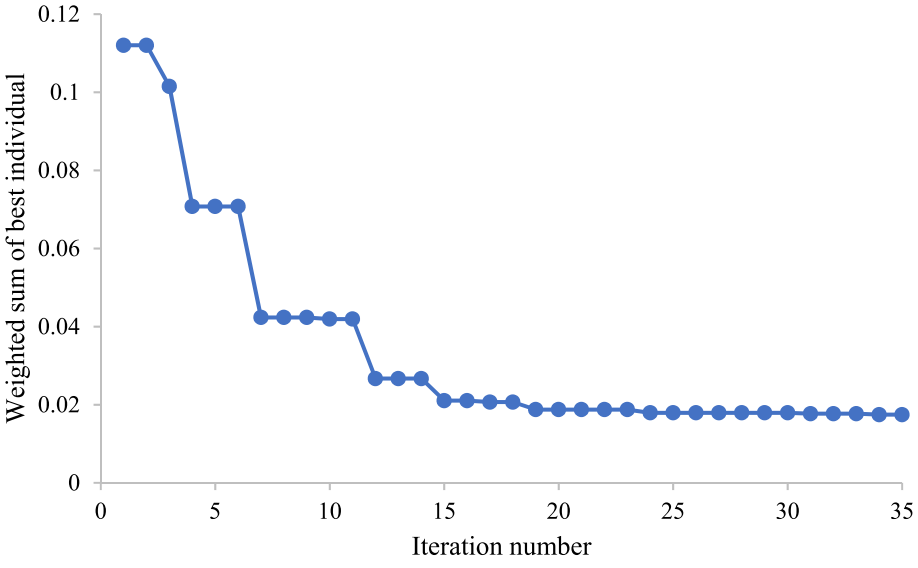

Fig. 10. Iteration-wise improvement example from pavement design 2 (baseline scenario) and ECI weight 0.5.

have their thicknesses defined in such a way that the design satisfies pavement performance criteria. In turn, the previously mentioned mixtures i.e., surface, lowest-positioned base and subbase mixtures, have always a thickness equal to the lower thickness boundary. The most common mixtures selected by the CMOO approach are mixtures 2, 3, 14, 18 and 19. This depends on a combination of two factors. First, the algorithm will favour a particular mixture because of the different ECI and construction costs associated with each mixture that are more suited for a given weighting set. Secondly, the required thickness of the in-between layers allows for a combination of different mixture-thickness possibilities in order to: 1) meet the OIA constraints, and, 2) minimize the weighted sum value for a given weighting set.

Further, the optimal solutions and corresponding constraint values show that the CMOO approach is in line with Bouman et al. (2012). This states that, for most cases, fatigue failure will occur before rutting failure. This alignment with the literature partly validates the verification of the constraint formulations in the CMOO approach.

It is worth mentioning the difference in restrictions applied to the pavement designer and CMOO approach for pavement design 5. The pavement designer must adhere to requirements set by the client i.e., the flexible pavement design should contain a certain number of layers with thicknesses specified beforehand. Additionally, the number of applicable mixtures to be used per layer is also limited, thereby creating limited design freedom for the pavement designer. On the other hand, the CMOO approach assumes complete design freedom. This allows for a cheaper and more environmentally sound design, as shown by reductions of the objective function values of 31% and 30%, respectively (for an ECI weight of 0), comparatively to the pavement designer approach.

Finally, pavement performance calculation requires data on physical properties of mixtures to be known. Such data is only known by the asphalt plant owner and contractor. Notwithstanding the lack of data for pavement performance calculation, it is the client who prescribes the flexible pavement design. This confirms the inefficient approach characterizing the decision-making process in the Dutch asphalt sector identified by the literature (Bijleveld et al., 2015; Miller et al., 2010). Such an approach can lead to over-designed road pavement structures and avoidable additional environmental impacts and construction costs, as is shown with pavement design 5.

6.2. Practical implications

From a practical point of view, the CMOO approach can be applied in a bidding procedure using the following steps. First, the input parameters including the mixtures dataset must be updated for the bid. Running the algorithm will result in one or several optimal solutions. The pavement designer can then choose one of the optimal solutions based on his/her preference for environmental and economic aspects.

Secondly, the chosen solution must be tested again in the actual OIA software to ensure that no over-design has occurred. The reason being that the optimal pavement structures defined by the CMOO approach are slightly thicker than the pavement structures obtained with the application of the OIA software. In the case of over-design, the optimal pavement structure can be fine-tuned until the over-design is overcome.

Finally, the optimal pavement structure should be sent to the contractor's sustainability department to calculate the detailed ECI and costs of the pavement design. ECI and costs include very detailed components that are not included in the CMOO approach.

6.3. Limitations of the CMOO approach

Obtaining the optimal pareto front for a set of 24 mixtures is already computationally expensive. If the size of dataset increases, the proposed GA parameter configuration would require recalibration. Both the recalibration process and new configuration itself most likely will require even higher computational times to maintain the optimization quality. A possible solution to decrease the computational time might be by pre-eliminating dominated mixtures from the dataset. Additional solutions for reducing the computational time can be found in the use of surrogate-based optimization (Gaurav et al., 2011) or Kriging meta-models (Dilip and Babu, 2021).

The calculation of pavement performance in the proposed CMOO approach does not consider the probabilistic nature of pavement design input parameters. Abed et al. (2019) argued that the variability of layer thickness and stiffness significantly impacted pavement performance. Therefore, ignoring uncertainties might result in under or over-designed pavement structure by the CMOO approach (Bhattacharjee, 2017; Luo et al., 2018). One way of tackling the stochasticity affecting the pavement design parameters might be to consider a reliability-based pavement design optimization approach (Dilip and Babu, 2021, 2023; Xin et al., 2021). This approach should be enhanced by considering the deterioration of the pavement over the design life by using a time-dependent reliability framework. In this way, pavement maintenance- and use-related costs and environmental impacts are also considered.

The current model formulations always assume a fixed subgrade material type, i.e., sand, where a subbase layer can be directly applied above the subgrade layer. In cases where the natural subgrade is a water-retaining material type, an additional sand layer is required between the subgrade and subbase layer. The current CMOO approach does not take this into account, but it can be upgraded to account for this situation. Hence, only project locations where sand is the natural subgrade layer are suitable for the current version of the proposed CMOO approach.

Finally, the algorithm can only assume a complete design freedom. That means that, if the client establishes beforehand any thickness- or mixture-related requirements, the CMOO approach becomes inapplicable. This also includes cases where the client requires a specified number of layers in the design. Additionally, only projects concerning complete reconstruction are suitable for the current version of the CMOO approach. Nevertheless, upgrading the CMOO approach to account for the pavement design circumstances previously mentioned can be accomplished without radical modifications.

7. Conclusions

The increasing number of possible flexible pavement design alternatives has made it difficult for pavement designers to find pavement designs that reduce both environmental impacts and construction costs, while also meeting pavement performance requirements. To solve this challenge, a CMOO approach has been developed that concomitantly minimizes environmental impacts and construction costs and uses a GA to find optimal pavement design solutions for different thickness-mixture combinations.

The proposed CMOO approach has been applied to five pavement designs with varying input parameters. The results show that the approach is able to find sets of optimal solutions for each pavement design. Additionally, one of these pavement designs was based on a real-life project, in which the original pavement design was compared with the optimal pavement design determined by the CMOO approach. The results show a considerable reduction in both environmental impacts (30% reduction) and construction costs (31% reduction).

Since pavement designers have little design freedom due to heavy requirements set by the client, the CMOO approach shows that a change in the traditional pavement design approach can be very beneficial to all parties involved. This implies that design responsibility should be handed over from the client to the contractor, since the latter has access to mixtures data and, therefore, it is in a more favourable position to design pavement structures that are less environmentally harmful and economically onerous.

Role of funding resources

This research did not receive any specific grant from funding agencies in the public, commercial, or not-for-profit sectors.

CRediT authorship contribution statement

Abrohom Demir: Conceptualization, Methodology, Software, Investigation, Writing – original draft, Visualization. **Joao Santos:** Conceptualization, Methodology, Resources, Writing – review & editing, Supervision, Project administration. **Seirgei Miller:** Conceptualization, Writing – review & editing, Supervision, Project administration. **Ronald Diele:** Conceptualization, Resources, Writing – review & editing, Supervision. **Gijs Naarding:** Supervision.

Declaration of competing interest

The authors declare that they have no known competing financial interests or personal relationships that could have appeared to influence the work reported in this paper.

Data availability

Data will be made available on request.

Acknowledgements

The author would like to thank TWW (Twentse Weg-en Waterbouw) and ReintenInfra for sharing their facilities and data used in the research work presented in this paper. Furthermore, the author would also like to thank Toni Messinella for the useful insights provided on the Dutch flexible pavement design procedure.

Appendix A

Table A1
Dataset considered in the application of the CMOO approach for the flexible pavement design problem

Mixture ID	Production plant	Mixture position	General mixture name	Thickness boundaries (mm)	Thickness step size (mm)	PC	PC_{base}	PC_{bind}	$PC_{bind,PA}$	C^{A1-3} (euro/ton)	ECI^{A1-3} (euro/ton)
1	1	Base/bind	AC 22 BASE/ BIND	55–90	5	N/A	1–4	1–4	1–3	60.74	4.52
2	1	Base/bind	AC 22 BASE/ BIND	55–90	5	N/A	1–4	1–4	2–4	55.42	4.14
3	1	Base/bind	AC 16 BASE/ BIND	40–60	5	N/A	1–4	1–4	2–4	55.08	3.81
4	1	Base/bind	AC 22 BASE/ BIND Mod.	55–90	5	N/A	1–4	1–4	2–4	64.58	4.78
5	2	Base/bind	AC 16 BASE/ BIND	40–60	5	N/A	1–4	2–3	2–4	49.82	4.20
6	2	Base/bind	AC 22 BASE/ BIND	55–90	5	N/A	1–4	2–3	2–4	49.82	4.20
7	2	Base/bind	AC 16 BASE/ BIND	40–60	5	N/A	1–4	2–3	2–4	48.31	4.28
8	2	Base/bind	AC 22 BASE/ BIND	55–90	5	N/A	1–4	2–3	2–4	48.31	4.28
9	1	Surface	AC 8 SURF	20–30	5	1–2	N/A	N/A	N/A	104.37	11.87
10	1	Surface	SMA-NL 8G	20–35	5	1–4	N/A	N/A	N/A	114.58	12.36
11	1	Surface	PA 16	50–60	5	1–4	N/A	N/A	N/A	103.46	11.37
12	1	Base/bind	AC 22 BASE/ BIND	55–90	5	N/A	1–4	1–4	1–3	59.10	5.18
13	1	Base/bind	AC 22 BASE/ BIND	55–90	5	N/A	1–4	1–4	2–4	53.79	4.97
14	1	Base/bind	AC 16 BASE/ BIND	40–60	5	N/A	1–4	1–4	2–4	53.45	4.67
15	1	Base/bind	AC 22 BASE/ BIND Mod.	55–90	5	N/A	1–4	1–4	2–4	62.94	5.64
16	2	Base/bind	AC 16 BASE/ BIND	40–60	5	N/A	1–4	2–3	2–4	43.81	4.62
17	2	Base/bind	AC 22 BASE/ BIND	55–90	5	N/A	1–4	2–3	2–4	43.81	4.62
18	2	Base/bind	AC 16 BASE/ BIND	40–60	5	N/A	1–4	2–3	2–4	42.31	4.80
19	2	Base/bind	AC 22 BASE/ BIND	55–90	5	N/A	1–4	2–3	2–4	42.31	4.80
20	1	Surface	AC 8 SURF	20–30	5	1–2	N/A	N/A	N/A	102.73	12.72
21	1	Surface	SMA-NL 8G	20–35	5	1–4	N/A	N/A	N/A	112.94	13.02
22	1	Surface	PA 16	50–60	5	1–4	N/A	N/A	N/A	101.82	12.00
23	3	Subbase	Mixed granulate	250–350	50	1–4	N/A	N/A	N/A	6.82	0
24	3	Subbase	Hydraulic mixed granulate	250–350	50	1–4	N/A	N/A	N/A	8.46	0.36

Mixture ID	ρ^1	Mixture type[2]	$c_1^{f\,1}$	$c_2^{f\,1}$	$c_3^{f\,1}$	$c_4^{f\,1}$	$c_5^{f\,1}$	$H_f{}^1$	$c_1^{E\,1}$	$c_2^{E\,1}$	$c_3^{E\,1}$	$c_4^{E\,1}$	$T^{E\,1}$	$f^{E\,1}$	$CK^{E\,1}$	E^1	Poisson's ratio
1	9	7	5	1	1	5	5	1	7	1	1	1	1	1	1	N/A	0.35
2	7	7	1	1	1	1	1	5	3	1	1	1	1	1	1	N/A	0.35
3	17	7	3	1	1	3	3	1	5	1	1	1	1	1	1	N/A	0.35
4	1	8	7	1	1	11	11	15	1	1	1	1	1	1	1	N/A	0.35

(*continued on next page*)

Table A1 (*continued*)

Mixture ID	ρ^1	Mixture type[2]	$c_1^{f\,1}$	$c_2^{f\,1}$	$c_3^{f\,1}$	$c_4^{f\,1}$	$c_5^{f\,1}$	$H_f{}^1$	$c_1^{E\,1}$	$c_2^{E\,1}$	$c_3^{E\,1}$	$c_4^{E\,1}$	$T^{E\,1}$	$f^{E\,1}$	$CK^{E\,1}$	E^1	Poisson's ratio
5	3	7	9	1	1	7	7	11	9	1	1	1	1	1	1	N/A	0.35
6	3	7	9	1	1	7	7	11	9	1	1	1	1	1	1	N/A	0.35
7	11	7	13	1	1	13	13	5	13	1	1	1	1	1	1	N/A	0.35
8	11	7	13	1	1	13	13	5	13	1	1	1	1	1	1	N/A	0.35
9	15	1	N/A	N/A	N/A	N/A	N/A	N/A	17	1	1	1	1	1	1	N/A	0.35
10	19	15	N/A	N/A	N/A	N/A	N/A	N/A	19	N/A	N/A	N/A	N/A	N/A	N/A	N/A	0.35
11	21	10	N/A	N/A	N/A	N/A	N/A	N/A	21	N/A	N/A	N/A	N/A	N/A	N/A	N/A	0.35
12	9	7	5	1	1	5	5	1	7	1	1	1	1	1	1	N/A	0.35
13	7	7	1	1	1	1	1	5	3	1	1	1	1	1	1	N/A	0.35
14	17	7	3	1	1	3	3	1	5	1	1	1	1	1	1	N/A	0.35
15	1	8	7	1	1	11	11	15	1	1	1	1	1	1	1	N/A	0.35
16	3	7	9	1	1	7	7	11	9	1	1	1	1	1	1	N/A	0.35
17	3	7	9	1	1	7	7	11	9	1	1	1	1	1	1	N/A	0.35
18	11	7	13	1	1	13	13	5	13	1	1	1	1	1	1	N/A	0.35
19	11	7	13	1	1	13	13	5	13	1	1	1	1	1	1	N/A	0.35
20	15	1	N/A	N/A	N/A	N/A	N/A	N/A	17	1	1	1	1	1	1	N/A	0.35
21	19	15	N/A	N/A	N/A	N/A	N/A	N/A	19	N/A	N/A	N/A	N/A	N/A	N/A	N/A	0.35
22	21	10	N/A	N/A	N/A	N/A	N/A	N/A	21	N/A	N/A	N/A	N/A	N/A	N/A	N/A	0.35
23	24	N/A	N/A	N/A	N/A	N/A	N/A	N/A	N/A	N/A	N/A	N/A	N/A	N/A	N/A	2	0.35
24	23	N/A	N/A	N/A	N/A	N/A	N/A	N/A	N/A	N/A	N/A	N/A	N/A	N/A	N/A	1	0.35

[1]Descending ranking order (from the highest to the lowest value).
[2]Mixture type based on Bak et al. (2022) for the cost and ECI calculations of LCA stage A5.

References

AASTHO, 1993. AASHTO Guide for Design of Pavement Structures. American Association of State Highway and Transportation Officials.

Abaza, K.A., 2021. Empirical-Markovian approach for estimating the flexible pavement structural capacity: Caltrans method as a case study. Int. J. Transp. Sci. Technol. 10 (2), 156–166. https://doi.org/10.1016/j.ijtst.2020.12.007.

Abaza, K.A., Abu-Eisheh, S.A., 2003. An optimum design approach for flexible pavements. Int. J. Pavement Eng. 4 (1), 1–11. https://doi.org/10.1080/1029843031000087464.

Abed, A., Thom, N., Neves, L., 2019. Probabilistic prediction of asphalt pavement performance. Road Mater. Pavement Des. 20, 247–264. https://doi.org/10.1080/14680629.2019.1593229.

Bai, Y., Gungor, O.E., Hernandez-Urrea, J.A., Ouyang, Y., Al-Qadi, I.L., 2015. Optimal pavement design and rehabilitation planning using a mechanistic-empirical approach. EURO J. Transp. Logist. 4 (1), 57–73. https://doi.org/10.1007/s13676-014-0072-2.

Bak, I., Overmars, L., Van der Kruk, T., 2022. LCA Achtergrondrapport Voor Nederlandse Branchereferentiemengsels 2022.

Bhattacharjee, S., 2017. Incorporating uncertainties in flexible pavement design. Proc. Inst. Civ. Eng.- Transp. 170 (3), 158–170. https://doi.org/10.1680/jtran.15.00031.

Bijleveld, F.R., Miller, S.R., Dorée, A.G., 2015. Making operational strategies of asphalt teams explicit to reduce process variability. J. Construct. Eng. Manag. 141 (5), 04015002 https://doi.org/10.1061/(ASCE)CO.1943-7862.0000969.

Bouman, S., Cuppens, G., Van Dommelen, A., Eijbersen, M., Van Gurp, C., Pouwels, M., Robbemond, P., Roos, H., Sluer, B., Thewessen, B., De Vries, J., Willemsen, M.-M., 2012. Achtegrondrapport Ontwerpinstrumentarium Asfaltverhardingen (OIA).

CROW, 2020. n.d.. In: Standaard RAW Bepalingen 2020. CROW.

De Bruyn, S., Ahdour, S., Bijleveld, M., De Graaff, L., Schep, E., Schroten, A., Vergeer, R., 2017. Environmental Prices Handbook 2017. CE Delft.

Deb, K., 2001. Multi-objective Optimization Using Evolutionary Algorithms, first ed. John Wiley & Sons.

Deb, K., 2011. In: Wang, L., Ng, A.H.C., Deb, K. (Eds.), Multi-objective optimisation using evolutionary algorithms: an introduction, Multi-objective Evolutionary Optimisation for Product Design and Manufacturing. Springer London, pp. 3–34. https://doi.org/10.1007/978-0-85729-652-8_1.

Deb, K., Pratap, A., Agarwal, S., Meyarivan, T., 2002. A fast and elitist multiobjective genetic algorithm: NSGA-II. IEEE Trans. Evol. Comput. 6 (2), 182–197. https://doi.org/10.1109/4235.996017.

Dilip, D.M., Babu, G.L.S., 2021. Reliability-based design optimization of flexible pavements using kriging models. J. Transport. Eng., Part B: Pav. 147 (3), 04021046 https://doi.org/10.1061/JPEODX.0000306.

Dilip, D.M., Babu, G.L.S., 2023. System reliability-based design optimization of flexible pavements using adaptive meta-modelling techniques. Construct. Build. Mater. 367, 130351 https://doi.org/10.1016/j.conbuildmat.2023.130351.

Ecochain Helix, 2022. Ecochain Technologies B.V.

Ecoinvent, 2020. Ecoinvent v3.5. https://ecoinvent.org/the-ecoinvent-database/data-releases/ecoinvent-3-5/.

Espinoza, M., Campos Campos, N., Yang, R., Ozer, H., Aguiar-Moya, J., Baldi Sevilla, A., Loria Salazar, L., 2019. Carbon footprint estimation in road construction: La Abundancia–Florencia case study. Sustainability 11, 2276. https://doi.org/10.3390/su11082276.

Ferreira, A., Santos, J., 2012. Pavement design optimization considering costs and preventive interventions. J. Transport. Eng. 138, 911–923. https://doi.org/10.1061/(ASCE)TE.1943-5436.0000390.

Garbarino, E., Rodriguez Quintero, Rocío, Donatello, S., Wolf, O., 2016. Revision of Green Public Procurement Criteria for Road Design, Construction and Maintenance: Procurement Practice Guidance Document. Publications Office.

Gaurav, G., Wojtkiewicz, S., Khazanovich, L., 2011. Optimal design of flexible pavements using a framework of Dakota and MEPDG. Int. J. Pav. Engi. 12, 137–148. https://doi.org/10.1080/10298436.2010.535535.

Ghanizadeh, A.R., 2016. An optimization model for design of asphalt pavements based on IHAP code number 234. Adv. Civ. Eng. 1–8. https://doi.org/10.1155/2016/5942342, 2016.

Hadi, M.N.S., Arfiadi, Y., 2001. Optimum rigid pavement design by genetic algorithms. Comput. Struct. 79 (17), 1617–1624. https://doi.org/10.1016/S0045-7949(01)00038-4.

Huang, Y.H., 2004. Pavement Analysis and Design, second ed. Pearson/Prentice Hall.

LaTorre, A., Molina, D., Osaba, E., Del Ser, J., Herrera, F., 2020. Fairness in Bio-Inspired Optimization Research: A Prescription of Methodological Guidelines for Comparing Meta-Heuristics (arXiv:2004.09969). arXiv. http://arxiv.org/abs/2004.09969.

Lee, J., Madanat, S., 2014. Joint optimization of pavement design, resurfacing and maintenance strategies with history-dependent deterioration models. Transp. Res. Part B Methodol. 68, 141–153. https://doi.org/10.1016/j.trb.2014.06.008.

Luo, Z., Karki, A., Pan, E., Abbas, A.R., Arefin, M.S., Hu, B., 2018. Effect of uncertain material property on system reliability in mechanistic-empirical pavement design. Construct. Build. Mater. 172, 488–498. https://doi.org/10.1016/j.conbuildmat.2018.03.236.

Mamlouk, M.S., Zaniewski, J.P., He, W., 2000. Analysis and design optimization of flexible pavement. J. Transport. Eng. 126 (2), 161–167. https://doi.org/10.1061/(ASCE)0733-947X(2000)126:2(161).

Matlab R2021b, 2021. The Mathworks, Inc.

McDonald, M., Madanat, S., 2012. Life-cycle cost minimization and sensitivity analysis for mechanistic-empirical pavement design. J. Transport. Eng. 138 (6), 706–713. https://doi.org/10.1061/(ASCE)TE.1943-5436.0000346.

Miettinen, K., 2008. In: Branke, J., Deb, K., Miettinen, K., Slowiński, R. (Eds.), Introduction to multiobjective optimization: noninteractive approaches, Multiobjective Optimization: Interactive and Evolutionary Approaches. Springer Berlin Heidelberg, pp. 1–26. https://doi.org/10.1007/978-3-540-88908-3_1.

Miettinen, K., 2012. Nonlinear Multiobjective Optimization, vol. 12. Springer Science & Business Media.

Miller, S., Huerne, H., Dorée, A., 2010. Role of action research in dealing with a traditional process, first ed. In: Performance Improvement in Construction Management. Routledge, pp. 92–101.

Miner, M.A., 1945. Cumulative damage in fatigue. J. Mech. Eng. 12 (3), 159–164.

Odemark, N., 1949. Investigations as to the Elastic Properties of Soils and Design of Pavements According to the Theory of Elasticity.

Peddinti, P.R.T., Munwar Basha, B., Saride, S., 2020. System reliability framework for design of flexible pavements. J. Transport. Eng., Part B: Pav. 146 (3), 04020043 https://doi.org/10.1061/JPEODX.0000186.

Pryke, A., Evdorides, H., Ermaileh, R.A., 2006. Optimization of pavement design using a genetic algorithm. In: 2006 IEEE International Conference on Evolutionary Computation, pp. 1095–1098. https://doi.org/10.1109/CEC.2006.1688431.

Rajbongshi, P., Das, A., 2008. Optimal asphalt pavement design considering cost and reliability. J. Transport. Eng. 134 (6), 255–261. https://doi.org/10.1061/(ASCE)0733-947X(2008)134:6(255).

Reeves, C.R., 2010. s. In: Gendreau, M., Potvin, J.-Y. (Eds.), Genetic algorithm, Handbook of Metaheuristics, vol. 146. Springer US, pp. 109–139. https://doi.org/10.1007/978-1-4419-1665-5_5.

Rijkswaterstaat, 2016. Specificaties Ontwerp Asfaltverhardinge. Rijkswaterstaat.

Sahis, M.K., Biswas, P.P., 2021. Optimization of bituminous pavement thickness using mechanistic-empirical strain-based design approach. Civ. Eng. J. 7 (5), 804–815. https://doi.org/10.28991/cej-2021-03091691.

Sanchez-Silva, M., Arroyo, O., Junca, M., Caro, S., Caicedo, B., 2005. Reliability based design optimization of asphalt pavements. Int. J. Pavement Eng. 6 (4), 281–294. https://doi.org/10.1080/10298430500445506.

Santos, J., Ferreira, A., Flintsch, G., 2016. An adaptive hybrid genetic algorithm for pavement management. In: 5th International Conference on Theory and Practice in Modern Computing, pp. 211–218.

Santos, J., Ferreira, A., Flintsch, G., Cerezo, V., 2017a. A multi-objective optimization approach for sustainable pavement management. In: Life-Cycle of Engineering Systems: Emphasis on Sustainable Civil Infrastructure. Taylor & Francis, pp. 365–372.

Santos, J., Ferreira, A., Flintsch, G., Cerezo, V., 2017b. Consideration of life cycle greenhouse gas emissions in optimal pavement maintenance programming: A comparison between single- and multi-objective optimization approaches. In: *WCPAM2017* -. World Conference on Pavement and Asset Management.

Santos, J., Ferreira, A., Flintsch, G., Cerezo, V., 2018. A multi-objective optimisation approach for sustainable pavement management. Struct. Infrastruct. Eng. 854–868. https://doi.org/10.1080/15732479.2018.1436571.

Saride, S., Peddinti, P.R.T., Basha, M.B., 2019. Reliability perspective on optimum design of flexible pavements for fatigue and rutting performance. J. Transport. Eng., Part B: Pav. 145 (2), 04019008 https://doi.org/10.1061/JPEODX.0000108.

Sivanandam, S.N., Deepa, S.N., 2008. Terminologies and operators of GA. In: Introduction to Genetic Algorithms. Springer London NetLibrary, Inc, pp. 39–81.

Skar, A., Andersen, S., 2020. ALVA: an adaptive MATLAB package for layered viscoelastic analysis. J. Open Source Softw. 5 (55), 2548. https://doi.org/10.21105/joss.02548.

Strickland, D., 2015. In: Hunter, R.N., Self, A., Read, J. (Eds.), Design of flexible pavements, sixth ed., The Shell Bitumen Handbook. ICE Publishing, pp. 347–377.

Talbi, E.-G., 2009. Metaheuristics: from Design to Implementation. John Wiley & Sons.

Van der Kruk, T., Overmars, L., 2022. Product Category Rules voor bitumineuze materialen in verkeersdragers en waterwerken in Nederland ("PCR Asfalt").

Vasudevan, J., Raju, S., Lu, J., 2015. In: Hunter, R.N., Self, A., Read, J. (Eds.), Properties of asphalts, sixth ed., The Shell Bitumen Handbook. ICE Publishing, pp. 479–501.

Xin, J., Akiyama, M., Frangopol, D.M., Zhang, M., Pei, J., Zhang, J., 2021. Reliability-based life-cycle cost design of asphalt pavement using artificial neural networks. Struct. Infrastruct. Eng. 17 (6), 872–886. https://doi.org/10.1080/15732479.2020.1815807.

Yu, X., Gen, M., 2010. Introduction to Evolutionary Algorithms, (Vol. 0).. Springer, London. https://doi.org/10.1007/978-1-84996-129-5.